

Experimental validation of the high-order coronagraphic phase diversity (COFFEE) on the SPHERE system

Baptiste Paul^{a,b,e}, Jean-François Sauvage^{a,c,e}, Laurent M. Mugnier^{a,e}, Kjetil Dohlen^{b,e}, David Mouillet^{c,e}, Thierry Fusco^{a,b,e}, Jean-Luc Beuzit^{c,e}, Mamadou N'Diaye^{d,e}, Marc Ferrari^{b,e}

^aOnera - The French Aerospace Lab, F-92322 Chatillon France.

^bLaboratoire d'Astrophysique de Marseille (LAM), Université Aix-Marseille/CNRS, 13388 Marseille Cedex 13, France.

^cInstitut de Planétologie et d'Astrophysique de Grenoble (IPAG), BP 53 F-38041 Grenoble Cedex 9, France.

^dSpace Telescope Science Institute, 3700 San Martin Drive, Baltimore MD 21218, USA.

^eGroupement d'intérêt scientifique PHASE (Partenariat Haute résolution Angulaire Sol et Espace) between Onera, Observatoire de Paris, CNRS, Université Diderot, Laboratoire d'Astrophysique de Marseille and Institut de Planétologie et d'Astrophysique de Grenoble.

ABSTRACT

The final performance of current and future instruments dedicated to exoplanet detection and characterization (such as SPHERE on the VLT, GPI on Gemini North or future instruments on the E-ELT) is limited by intensity residuals in the scientific image plane, which originate in uncorrected optical aberrations. After correction of the atmospheric turbulence, the main contribution to these residuals comes from the quasi-static aberrations introduced upstream of the coronagraph. In order to measure and compensate for these aberrations, we propose a dedicated focal-plane sensor called COFFEE (for COronagraphic Focal-plane wave-Front Estimation for Exoplanet detection), which consists in an extension of conventional phase diversity to a coronagraphic system: aberrations both upstream and downstream of the coronagraph are estimated using two coronagraphic focal-plane images, recorded from the scientific camera itself, without any differential aberration. This communication gathers COFFEE's improvements: the phase estimation is performed on a pixel-wise map coupled with a dedicated regularization metric. This allows COFFEE to estimate very high order aberrations, making possible to estimate and compensate for quasi-static aberrations with nanometric precision, leading to an optimization of the contrast on the scientific detector in the whole AO corrected area. Besides, COFFEE has been modified so that it can be used with any coronagraphic focal plane mask. Lastly, we use COFFEE to measure and correct the wavefront on the SPHERE (Spectro-Polarimetric High-contrast Exoplanet Research) instrument during its integration phase: COFFEE's estimation is used to compensate for the quasi-static aberrations upstream of the coronagraph, leading to a contrast improvement on the scientific camera.

Keywords: wave-front sensing, inverse problem, high contrast imaging, phase diversity, exoplanet detection

1. INTRODUCTION

The observation of an extremely faint object such as an exoplanet very close to its parent star requires the use of an extreme adaptive optics (XAO) system coupled with a high-contrast imaging technique such as coronagraphy. The current generation of instruments dedicated to exoplanets direct imaging (SPHERE on the VLT,¹ GPI on Gemini North²) aim at detecting massive gaseous planets 10^6 to 10^7 times fainter than their host star.

The ultimate limitation of a high-contrast imaging instrument lies in its quasi-static non-common path aberrations (NCPA): these aberrations, uncorrected by the AO loop, create speckles on the detector plane,³ limiting the achievable contrast. Besides, these long-lived speckles can easily be mistaken for a planet. Thus, in order to reach the instrument ultimate performance, these aberrations upstream of the coronagraph must be estimated and compensated for.

Further author information: (Send correspondence to B. Paul)

B. Paul: E-mail: baptiste.paul@onera.fr, Telephone: +33 (0)1 46 73 94 10

Several techniques dedicated to this goal have been proposed. Closed loop methods, which assume small aberrations,^{4,5} estimate the electric field in the detector plane using at least three images. The technique proposed by Baudoz *et al.*⁶ relies on a modification of the imaging system, but requires only one image.

The focal plane wave-front sensor we propose,⁷ called COFFEE (for COronagraphic Focal-plane wave-Front Estimation for Exoplanet detection), requires only two focal-plane images to estimate the aberrations upstream of the coronagraph without any modification of the coronagraphic imaging system or assuming small aberrations. We have adapted COFFEE to make it able to estimate high-order aberrations for any coronagraphic device.⁸ Such improvements are recalled in Section 2. Section 3 present the experimental validation of COFFEE on the SPHERE instrument. In particular, we demonstrate the ability to optimize the contrast on the detector plane using COFFEE’s estimation to compensate for the aberrations upstream of the coronagraph. Section 4 concludes the paper.

2. HIGH-ORDER CORONAGRAPHIC PHASE DIVERSITY

COFFEE’s used to be limited by both aliasing and the modelling error.⁹ The former was due to the use of a Zernike basis and prevent COFFEE from estimating high order aberrations. Moreover, the estimation of these high order aberrations is mandatory to optimize the contrast in the detector far from the optical axis. The latter was originating in the image formation model used by COFFEE. The estimations were indeed performed using a perfect coronagraph model, and thus limited by a model error. In practice, COFFEE’s use was limited to the apodized Roddier & Roddier coronagraph.

In order to get rid of these two limitations, we have developed a new version of COFFEE, which is able to estimate for high-order aberrations.⁸ Section 2.1 recall the modification of the maximum *a posteriori* (MAP) approach on which COFFEE is based, which includes a modification of the basis used for the aberration estimation, now composed of pupil indicator functions (pixels). Besides, a modification of the image formation model, described in Section 2.2, allows COFFEE to work with any coronagraphic device. Performances of this high-order version of COFFEE are assessed by a realistic simulation, performed in the SPHERE framework in Section 2.3.

2.1 Criterion expression

We consider a coronagraphic imaging system, presented on Figure 1, made of four successive planes denoted by A (circular entrance pupil of diameter D_u), B (coronagraphic focal plane), C (Lyot Stop), and D (detector plane). The optical aberrations are considered as static and introduced in pupil planes A and C. The coronagraphic device is composed of a focal plane mask located in plane B and a Lyot Stop in plane C. No particular assumption is made on the pupil shape or intensity, which can be calibrated using data recorded from the instrument. COFFEE requires only two images i_c^{foc} and i_c^{div} recorded on the detector (plane D) that, as in phase diversity, differ from a known aberration ϕ_{div} , to estimate aberrations both upstream (ϕ_u) and downstream (ϕ_d) of the coronagraph.

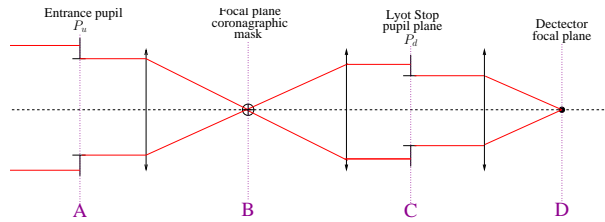


Figure 1. Principle of a Coronagraphic imaging instrument.

Considering the calibration of the instrument with an unresolved object, we use the following imaging model:

$$\begin{aligned} i_c^{\text{foc}} &= \alpha_{\text{foc}} h_{\text{det}} \star h_c(\phi_u, \phi_d) + n_{\text{foc}} + \beta_{\text{foc}} \\ i_c^{\text{div}} &= \alpha_{\text{div}} h_{\text{det}} \star h_c(\phi_u + \phi_{\text{div}}, \phi_d) + n_{\text{div}} + \beta_{\text{div}} \end{aligned} \quad (2.1)$$

where α_p is the incoming flux (p is for “foc” or “div”), h_c the coronagraphic “point spread function” (PSF) of the instrument (which is the response of a coronagraphic imaging system to a point source), h_{det} the known detector PSF, n_{foc}

and \mathbf{n}_{div} are the measurement noises and include both detector and photon noises, β_p is a unknown uniform background (offset), and \star denotes the discrete convolution operation.

COFFEE is based on a maximum *a posteriori* (MAP) approach: it estimates the aberrations ϕ_u and ϕ_d as well as the fluxes $\alpha = [\alpha_{\text{foc}}, \alpha_{\text{div}}]$, and the residual backgrounds $\beta = [\beta_{\text{foc}}, \beta_{\text{div}}]$ that minimize the neg-log-likelihood of the data, penalized by regularization terms $\mathcal{R}(\phi_u)$ and $\mathcal{R}(\phi_d)$ designed to enforce smoothness of the sought phases:

$$(\hat{\alpha}, \hat{\beta}, \hat{\phi}_u, \hat{\phi}_d) = \arg \min_{\alpha, \beta, \phi_u, \phi_d} [J(\alpha, \beta, \phi_u, \phi_d)] \quad (2.2)$$

where

$$\begin{aligned} J(\alpha, \beta, \phi_u, \phi_d) = & \frac{1}{2} \left\| \frac{\mathbf{i}_c^{\text{foc}} - (\alpha_{\text{foc}} \mathbf{h}_{\text{det}} \star \mathbf{h}_c(\phi_u, \phi_d) + \beta_{\text{foc}})}{\sigma_n^{\text{foc}}} \right\|^2 \\ & + \frac{1}{2} \left\| \frac{\mathbf{i}_c^{\text{div}} - (\alpha_{\text{div}} \mathbf{h}_{\text{det}} \star \mathbf{h}_c(\phi_u + \phi_d, \phi_d) + \beta_{\text{div}})}{\sigma_n^{\text{div}}} \right\|^2 \\ & + \mathcal{R}(\phi_u) + \mathcal{R}(\phi_d) \end{aligned} \quad (2.3)$$

where $\|x\|^2$ denotes the sum of squared pixel values of map x , σ_n^{foc} , and σ_n^{div} are the noise standard deviation maps of each image. The corresponding variance can be computed as a sum of the photon and detector noise variance. The former can be estimated as the image itself thresholded to positive values, and the latter can be calibrated prior to the estimation.

Both aberrations ϕ_u and ϕ_d are expanded on a basis $\{\mathbf{b}_k\}$. As described in Paul *et al.*,⁸ the use of a pixel indicator basis ($\phi = \sum_k p_k \mathbf{b}_k$) allows the estimation of high order aberrations. Besides, the use of such a basis strongly reduces the aliasing error. Since a pixel basis leads to a large number of unknowns, it is mandatory to perform the criterion minimization with an adapted regularization metric in order to reduce the noise sensitivity. This regularization metric is based on the available *a priori* knowledge on the quasi-static aberrations, assumed to be endowed with a power spectral density (PSD) S_{ϕ_k} (where k stands for u (upstream) or d (downstream)) which decreases as $1/\nu^2$ (with ν the spatial frequency). Such an assumption corresponds to a classical assumption for mirror fabrication errors. The regularization metric $\mathcal{R}(\phi_k)$ can thus be expressed as:⁸

$$\mathcal{R}(\phi_k) = \frac{1}{2\sigma_{\nabla\phi_k}^2} \|\nabla\phi_k(r)\|^2. \quad (2.4)$$

The minimization of metric $J(\alpha, \beta, \phi_u, \phi_d)$ of Eq. (2.3) is performed by means of a limited memory variable metric (BFGS) method,^{10,11} which is a fast quasi-Newton type minimization method. It uses gradients $\frac{\partial J}{\partial \phi_u}$, $\frac{\partial J}{\partial \phi_d}$, $\frac{\partial J}{\partial \alpha}$ and $\frac{\partial J}{\partial \beta}$ to estimate ϕ_u , ϕ_d , α and β .

In a previous paper,⁸ we established that a suitable diversity phase ϕ_{div} for COFFEE was a mix of defocus and astigmatism: $\phi_{\text{div}} = a_4^{\text{div}} Z_4 + a_5^{\text{div}} Z_5$ with $a_4^{\text{div}} = a_5^{\text{div}} = 0.8$ rad RMS, introduced upstream of the coronagraph.

2.2 Coronagraphic image formation model

To perform the minimization of criterion J in Eq. (2.3), the image formation model used by COFFEE (Equation (2.1)) requires the expression of a coronagraphic PSF h_c . Let r be the pupil plane position vector and γ the focal plane position vector. the entrance pupil function P_u is such that:

$$P_u(r) = \Pi \left(\frac{2r}{D_u} \right) \Phi(r), \quad (2.5)$$

with Π the disk of unit radius, D_u the entrance pupil diameter, and Φ a known apodization function. The electric field in the entrance pupil can be written as:

$$\Psi_A(r) = P_u(r) e^{j\phi_u(r)}. \quad (2.6)$$

The electric field in the detector plane Ψ_D is obtained by propagating Ψ_A through each plane of the coronagraphic imaging system: the signal is first focused on the coronagraphic focal plane mask \mathcal{M} ; then, the electric field is propagated trough

the Lyot Stop pupil $P_d(r)$ ($P_d(r) = \Pi(2r/D_d)$ with D_d the Lyot Stop pupil diameter). The electric field in the detector plane Ψ_D can thus be written as:

$$\Psi_d(\gamma) = \mathcal{F}^{-1} \left\{ \mathcal{F} \left[\mathcal{F}^{-1} (\Psi_A(r)) \mathcal{M} \right] P_d(r) e^{j\phi_d(r)} \right\}, \quad (2.7)$$

where \mathcal{F}^{-1} is the inverse Fourier transform operation. For the sake of simplicity, spatial variables r and u will be omitted in the following.

The coronagraphic PSF h_c is the square modulus of Ψ_D :

$$h_c = \left| \mathcal{F}^{-1} \left\{ \mathcal{F} \left[\mathcal{F}^{-1} (\Psi_A) \mathcal{M} \right] P_d e^{j\phi_d} \right\} \right|^2 \quad (2.8)$$

In Equation (2.8), \mathcal{M} can easily be adapted to represent any coronagraphic device, allowing COFFEE to be used with any high contrast imaging instrument.

2.3 Performance assessment by simulation

In this Section, we present COFFEE's performances using a realistic simulation, performed using the parameters gathered in Table 1

image size	$60 \times 60 \frac{\lambda}{D}$ (200×200 pixels, oversampling factor 1.69)
Light spectrum	Monochromatic, wavelength $\lambda = 1589$ nm
Entrance pupil	$D_u = 60$ pixels
Lyot stop pupil	$D_d = D_u$
Aberration upstream of the coronagraph (ϕ_u)	WFE _u = 50 nm RMS
Aberration downstream of the coronagraph (ϕ_d)	WFE _d = 20 nm RMS
Coronagraph	Apodized Lyot Coronagraph (ALC), focal plane mask angular diameter $d = 4.52\lambda/D$
Incoming flux	$\alpha = 10^9$ photons
Noise	Photon noise, detector noise ($\sigma_{e^-} = 1 e^-$)

Table 1. COFFEE: simulation parameters

These parameters have been chosen so that the following simulations are representative of the SPHERE instrument. The chosen coronagraph (ALC) is the one designed for the considered wavelength on SPHERE, and the apodization function used in the image formation model is the one designed for this coronagraph.

In order to evaluate COFFEE's performances, we define the reconstruction error ϵ_k as the WFE of the residual phase $\phi_k - \hat{\phi}_k$, where ϕ_k is the simulated aberration and $\hat{\phi}_k$ is the aberration estimated by COFFEE. From the randomly generated aberrations ϕ_u and ϕ_d , we compute two coronagraphic images, a focused one (i_{foc}) and a diversity one (i_{div}) using the image formation model of Eq. (2.1). Then, COFFEE use two two images to estimate the aberrations upstream and downstream of the coronagraph. Figure 2 present the result of such a reconstruction.

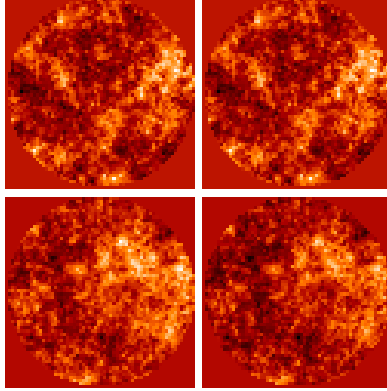


Figure 2. Top: Upstream aberration simulated (left) and estimated (right) by COFFEE (reconstruction error: $\epsilon_u = 1.78$ nm RMS). Bottom: Downstream aberration simulated (left) and estimated (right) by COFFEE (reconstruction error: $\epsilon_d = 3.85$ nm RMS). Same dynamic for all images.

The small values of reconstruction errors for both upstream and downstream aberrations estimation shows the quality of the estimation performed by COFFEE. Indeed, one can see on figure 2 that the estimated aberrations (right) are very close to the randomly generated ones (left).

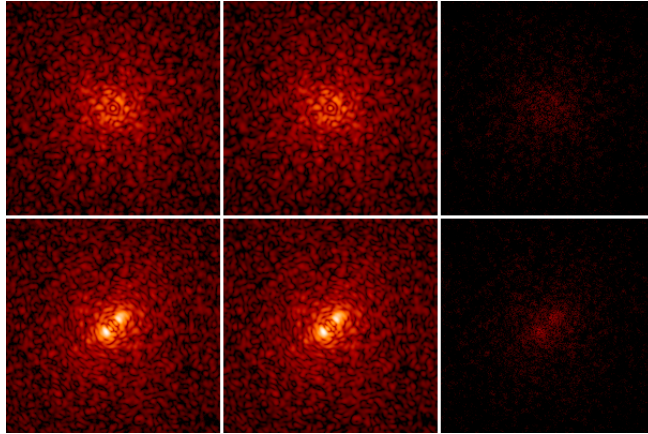


Figure 3. From left to right: coronagraphic images i_{foc} (top) and i_{div} (bottom) computed from the randomly generated aberrations ϕ_u and ϕ_d , coronagraphic images \hat{i}_{foc} (top) and \hat{i}_{div} (bottom) computed from the estimated aberrations $\hat{\phi}_u$ and $\hat{\phi}_d$, differences $|i_{\text{foc}} - \hat{i}_{\text{foc}}|$ (top) and $|i_{\text{div}} - \hat{i}_{\text{div}}|$ (bottom). Logarithmic scale, same dynamic for all images.

The quality of this estimation result, in turn, in a very good match between the coronagraphic images i_{foc} and i_{div} computed from ϕ_u and ϕ_d and the images \hat{i}_{foc} and \hat{i}_{div} computed from $\hat{\phi}_u$ and $\hat{\phi}_d$, as presented on figure 3, where no speckles remains in the difference between the images computed from the generated aberrations and the one computed using COFFEE's estimation. Most of all, the aberration phase map upstream of the coronagraph has been very well estimated.

3. APPLICATION TO THE SPHERE INSTRUMENT

COFFEE has been applied to the SPHERE instrument during its final integration phase in Grenoble. In Section 3.1, we briefly describe the experimental setup of the bench. Section 3.2 present the result of the estimation of a high-order aberration introduced upstream of the coronagraph using the deformable mirror (DM). Lastly, in Section 3.3, COFFEE's estimation is used to compensate for the aberrations upstream of the coronagraph in a closed-loop process.

3.1 Experimental setup

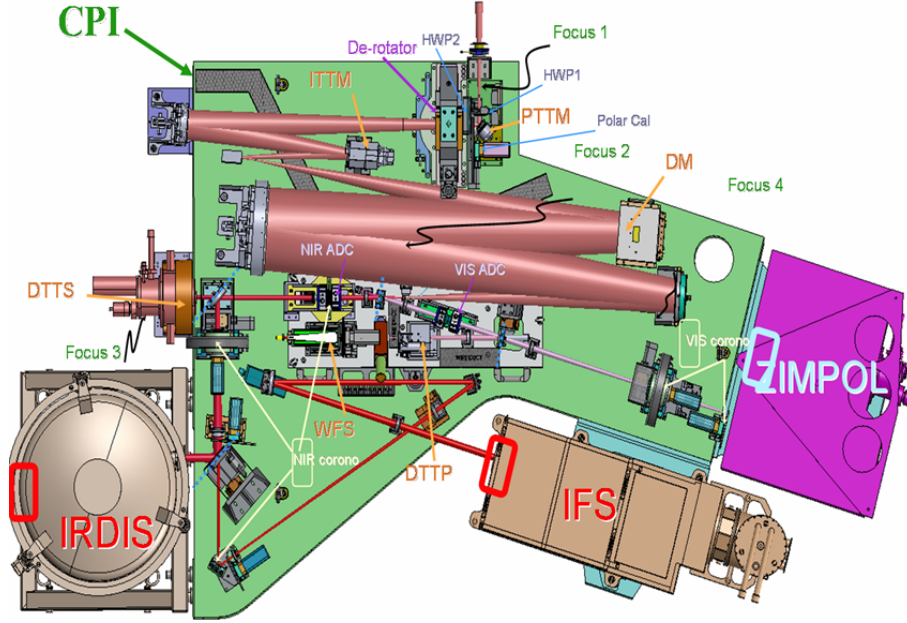


Figure 4. The SPHERE instrument

The SPHERE system,¹ presented on figure 4, is designed for the direct imaging of young giant extra-solar planets from the ground. This instrument includes an extreme adaptive optics (XAO) system, SAXO,¹² for the atmospheric turbulence compensation. The main limitation of this instrument lies in the non-common path quasi-static aberrations (named hereafter NCPA). To compensate for these aberrations, SPHERE's baseline relies on a differential estimation performed with phase diversity,¹³ a focal plane wave-front sensor that works with classical imaging (no coronagraph). It is noteworthy no mention that this wave-front sensor is limited to the estimation of aberrations up to 8 cycles per pupil (which only impact close to optical axis), whereas the XAO system could easily compensate up to 20 cycles per pupil.

Using the high-order version of COFFEE presented in this paper instead of classical phase diversity to compensate for SPHERE's NCPA would allow to estimate and compensate for high-order aberrations, leading to a contrast optimization far from the optical axis. Besides, since COFFEE is now able to work with any coronagraphic focal plane mask, one pair of images is enough to estimate the aberrations upstream of the coronagraph, instead of the two pairs required by the current baseline.

The coronagraphic images used by COFFEE are recorded from the near infrared detector IRDIS.¹⁴ Table 2 gather the parameters used for COFFEE experimental validation:

image size	$60 \times 60 \lambda/D$ (200 × 200 pixels, oversampling factor 1.69)
Light spectrum	Monochromatic, wavelength $\lambda = 1589$ nm
Entrance pupil	diameter D_u , no central obstruction, apodizer in the pupil
Lyot stop pupil	diameter $D_d = 0.96D_u$, central obstruction (15%)
Coronagraph	Apodized Lyot Coronagraph (ALC), focal plane mask angular diameter $d = 4.52\lambda/D$
Detector noise	$\sigma_{e^-} = 15 e^-$
Integration time	0.6 s
Number of image averaged for COFFEE's estimation	100

Table 2. Parameters of the experimental validation of COFFEE on the SPHERE system

In order to record the diversity image, the diversity phase is introduced upstream of the coronagraph by modifying the reference slopes of the XAO loop, using a method similar to the one described by Paul *et al.*⁹

3.2 NCPA measurement

In this section, we introduce a calibrated aberration upstream of the coronagraph by pushing (amplitude 144 nm PV) on an actuator of the 41×41 high-order deformable mirror of the XAO loop, creating a high order aberration (called hereafter a poke) in the DM pupil plane. This aberration is then estimated by COFFEE, using two focal plane coronagraphic images (focused and diversified).

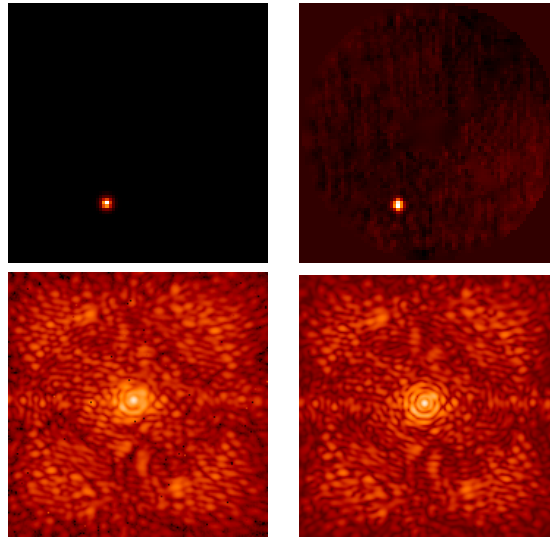


Figure 5. Estimation of a poke with COFFEE. Top: introduced poke (left), amplitude 144 nm PV and COFFEE estimated poke (right), amplitude 147 nm PV. Bottom: coronagraphic image recorded from SPHERE (left) and computed image using the estimated aberration (right).

Figure 5 shows the result of the poke estimation. As for the simulation, the accuracy of the estimation performed by COFFEE leads to a good match between the experimental image and the image computed using COFFEE's estimation (Figure 5, bottom).

3.3 Closed-loop process

Lastly, COFFEE's ability to compensate for the aberrations upstream of the coronagraph is demonstrated on the SPHERE instrument. To perform such an operation, we use a method named hereafter the Pseudo-Closed Loop (PCL) process.^{9,15} This iterative process, which aims at modifying the reference slopes of SAXO (whose thorough description has been performed by C. Petit *et al.*¹⁶), is described below: for the PCL iteration i :

1. acquisition of the focused i_{foc} and diverse i_{div} images;
2. estimation of the aberration $\hat{\phi}_u^i$ upstream of the coronagraph;
3. computation of the corresponding reference slopes correction $\delta s_i = g\mathcal{M}\hat{\phi}_u^i$, where g is the PCL gain. \mathcal{M} is a matrix which represent the linear transformation that allows to compute slopes from a given aberration. This matrix can easily be computed from the XAO loop matrices.
4. the AO loop is closed on the modified reference slopes.

The computation time required for one PCL iteration is typically 6 minutes, allowing us to compensate for quasi-static aberrations upstream of the coronagraph.

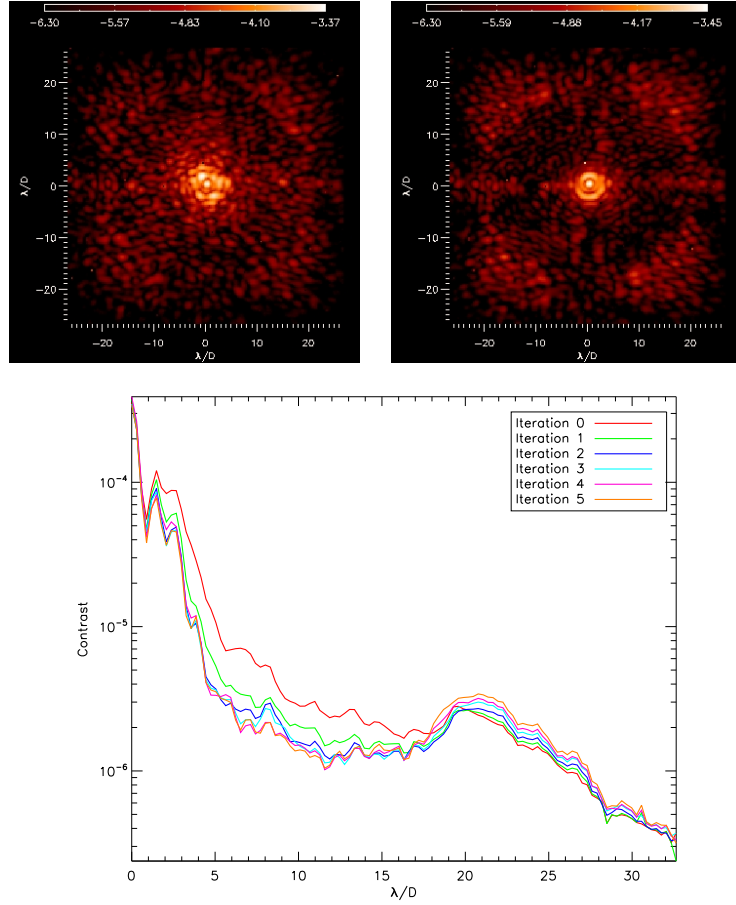


Figure 6. SPHERE NCPA upstream of the coronagraph compensation using COFFEE ($g = 0.5$). Top: coronagraphic images recorded from IRDIS before compensation (left) and after 5 iterations of the PCL (right). Logarithmic scale for both images. Bottom: average raw contrast profiles for each iteration (iteration 0: before compensation).

Figure 6 present the results obtained after 5 iterations of the PCL. On this figure, one can see that the compensation of the aberrations upstream of the coronagraph allows to remarkably remove speckles in the coronagraphic images (figure 6, top) in the whole detector plane area controlled by the AO loop. The average raw contrasts are computed from the coronagraphic images. Their plot (figure 6, bottom) clearly shows a contrast improvement in the focal plane when the number of iterations increases. As it has been said previously, classical phase diversity (which is the current SPHERE baseline) is unable to estimate frequencies higher than $8\lambda/D$. As one can clearly see on figure 6, the estimation performed by COFFEE, which includes high-order aberrations, allows to improve the contrast up to $18\lambda/D$. On Figure 6 (bottom), one can notice that beyond $18\lambda/D$, the incoming energy on the detector is increasing. This behavior seems to originate in the DM central actuators, which are not controlled the same way than the others actuators, since they will be located under the telescope central obstruction. It is noteworthy to mention that this increasing of high-order speckles does no longer appear when there is a central obscuration in the entrance pupil.

4. CONCLUSION

In this paper, an extended version of our coronagraphic phase diversity, nicknamed COFFEE, has been presented. The use of a regularized pixel basis in the estimation (Section 2) allows COFFEE to estimate high order aberrations with nanometric precision (Section 2.3). This high-order version of COFFEE has been successfully validated on the SPHERE instrument during its final integration phase (Section 3): in this paper, we demonstrated the ability of COFFEE to estimate high-order aberrations in Section 3.2, and Section 3.3 described the closed loop process, where COFFEE's estimation is used to improve the contrast on the detector.

Further developments of COFFEE will include a joint estimation of the amplitude aberrations, mandatory to reach a very high contrast level, such as the one required for the detection of earth-like planets. Besides, COFFEE can be extended to work on ground-based, long exposure images with residual turbulence induced aberrations. Another perspective lies in the optimization of the computation time required by COFFEE to estimate the aberrations. Such developments will eventually allow COFFEE to work on-line, during the scientific exposure.

Acknowledgments

The authors would like to thank the Région Provence-Alpes-Côte d'Azur for partial financial support of B. Paul's scholarship. This work was partly funded by the European Commission under FP7 Grant Agreement No. 312430 Optical Infrared Coordination Network for Astronomy.

REFERENCES

- [1] Beuzit, J.-L., Feldt, M., Dohlen, K., Mouillet, D., Puget, P., Antici, J., Baudoz, P., Boccaletti, A., Carbillet, M., Charton, J., Claudi, R., Fusco, T., Gratton, R., Henning, T., Hubin, N., Joos, F., Kasper, M., Langlois, M., Moutou, C., Pragt, J., Rabou, P., Saisse, M., Schmid, H. M., Turatto, M., Udry, S., Vakili, F., Waters, R., and Wildi, F., "SPHERE: A Planet Finder Instrument for the VLT," in [*Proceedings of the conference In the Spirit of Bernard Lyot: The Direct Detection of Planets and Circumstellar Disks in the 21st Century.*], Kalas, P., ed., University of California (June 2007).
- [2] Macintosh, B. A., Graham, J. R., Palmer, D. W., Doyon, R., and et al., J. D., "the gemini planet imager: from science to design to construction," in [*Adaptive Optics Systems*], **7015**, Proc. Soc. Photo-Opt. Instrum. Eng. (July 2008).
- [3] Soummer, R., Ferrari, A., Aime, C., and Jolissaint, L., "Speckle noise and dynamic range in coronagraphic images," *Astrophys. J.* **669** (November 2007).
- [4] Bordé, P. J. and Traub, W. A., "High contrast imaging from space : speckle-nulling in a low-aberration regime," *Astrophys. J.* **638** (February 2006).
- [5] Give'on, A., Belikov, R., Shaklan, S., and Kasdin, J., "Closed loop, DM diversity based, wave-front correction algorithm for high contrast imaging systems," *Opt. Express* **15** (2007).
- [6] Baudoz, P., Boccaletti, A., Baudrand, J., and Rouan, D., "The self-coherent camera : a new tool for exoplanet detection," in [*Proc. IAU Colloquium*], (2006).
- [7] Sauvage, J.-F., Mugnier, L., Paul, B., and Villicroze, R., "Coronagraphic phase diversity: a simple focal plane sensor for high-contrast imaging," *Opt. Lett.* **37**, 4808–4810 (Dec. 2012).
- [8] Paul, B., Mugnier, L. M., Sauvage, J.-F., and Dohlen, K., "High-order myopic coronagraphic phase diversity (COFFEE) for wave-front control in high-contrast imaging systems," *Opt. Express* (submitted).
- [9] Paul, B., Sauvage, J.-F., and Mugnier, L. M., "Coronagraphic phase diversity: performance study and laboratory demonstration," *Astron. Astrophys.* **552** (Apr. 2013).
- [10] Press, W. H., Teukolsky, S. A., Vetterling, W. T., and Flannery, B. P., [*Numerical Recipes : the art of scientific computing*], Cambridge University Press (2007).
- [11] Thiébaud, E., "Optimization issues in blind deconvolution algorithms," in [*Astronomical Data Analysis II*], **4847**, 174–183, Proc. Soc. Photo-Opt. Instrum. Eng. (December 2002).
- [12] Fusco, T., Rousset, G., Sauvage, J.-F., Petit, C., Beuzit, J.-L., Dohlen, K., Mouillet, D., Charton, J., Nicolle, M., Kasper, M., and Puget, P., "High order adaptive optics requirements for direct detection of extra-solar planets. application to the sphere instrument.," *Opt. Express* **14**(17), 7515–7534 (2006).
- [13] Sauvage, J.-F., Fusco, T., Petit, C., Mugnier, L., Paul, B., and Costille, A., "Focal-plane wave front sensing strategies for high contrast imaging: experimental validations on SPHERE," in [*Adaptive Optics Systems III*], Ellerbroek, B. L., Marchetti, E., and Véran, J.-P., eds., **8447**, 844715–844715–11, Proc. Soc. Photo-Opt. Instrum. Eng. (July 2012).
- [14] Langlois, M., Dohlen, K., Angereau, J.-C., Mouillet, D., Boccaletti, A., and Schmid, H.-M., "High contrast imaging with IRDIS near infrared polarimeter," in [*Ground-based and Airborne Instrumentation for Astronomy III*], **7735**, Proc. Soc. Photo-Opt. Instrum. Eng. (2010).
- [15] Sauvage, J.-F., Fusco, T., Rousset, G., and Petit, C., "Calibration and Pre-Compensation of Non-Common Path Aberrations for eXtreme Adaptive Optics," *J. Opt. Soc. Am. A* **24**, 2334–2346 (Aug. 2007).

- [16] Petit, C., Sauvage, J.-F., Sevin, A., Costille, A., Fusco, T., Baudoz, P., Beuzit, J. -L., Buey, T., Charton, J., Dohlen, K., Feautrier, P., Fedrigo, E., Gach, J.-L., Hubin, N., Hugot, E., Kasper, M., Mouillet, D., Perret, D., Puget, P., Siquin, J.-C., Soenke, C., Suarez, M., and Wildi, F., “The SPHERE XAO system SAXO: integration, test and laboratory performance,” in [*Adaptive Optics Systems III*], **8447**, Proc. Soc. Photo-Opt. Instrum. Eng. (2012).